

# Gating of myotonic Na channel mutants defines the response to mexiletine and a potent derivative

J.-F. Desaphy, PhD; A. De Luca, PhD; P. Tortorella, PhD; D. De Vito, PhD; A.L. George, Jr., MD; and D. Conte Camerino, PhD

**Article abstract**—*Background:* Myotonia and periodic paralysis caused by sodium channel mutations show variable responses to the anti-myotonic drug mexiletine. *Objective:* To investigate whether variability among sodium channel mutants results from differences in drug binding affinity or in channel gating. *Methods:* Whole-cell sodium currents ( $I_{Na}$ ) were recorded in tsA201 cells expressing human wild-type (WT) and mutant skeletal muscle sodium channels (A1156T, hyperkalemic periodic paralysis; R1448C, paramyotonia congenita; G1306E, potassium-aggravated myotonia). *Results:* At a holding potential (hp) of  $-120$  mV, mexiletine produced a tonic (TB, 0.33 Hz) and a use-dependent (UDB, 10 Hz) block of peak  $I_{Na}$  with a potency following the order rank R1448C > WT  $\approx$  A1156T > G1306E. Yet, when assayed from an hp of  $-180$  mV, TB and UDB by mexiletine were similar for the four channels. The different midpoints of channel availability curves found for the four channels track the half-maximum inhibitory value ( $IC_{50}$ ) measured at  $-120$  mV. Thus differences in the partitioning of channels between the closed and fast-inactivated states underlie the different  $IC_{50}$  measured at a given potential. The mexiletine-derivative, Me7 ( $\alpha$ -[2-methylphenoxy)methyl]-benzenemethanamine), behaved similarly but was  $\sim 5$  times more potent than mexiletine. Interestingly, the higher drug concentrations ameliorated the abnormally slower decay rate of myotonic  $I_{Na}$ . *Conclusions:* These results explain the basis of the apparent difference in block of mutant sodium channels by mexiletine and Me7, opening the way to a more rationale drug use and to design more potent drugs able to correct specifically the biophysical defect of the mutation in individual myotonic patients.

NEUROLOGY 2001;57:1849–1857

Paramyotonia congenita (PMC), potassium-aggravated myotonias (PAM), hyperkalemic periodic paralysis (hyperPP), and a second form of hypokalemic periodic paralysis (hypoPP2), are a set of dominantly inherited skeletal muscle disorders, all due to missense mutations in the *SCN4A* gene encoding the  $\alpha$ -subunit of the human skeletal muscle sodium channel (hSkM1).<sup>1,2</sup> Distinction between the four clinical entities is based on the presence of muscle weakness or stiffness and the nature of exacerbating factors. Although hypoPP2 mutations induce a loss of function of the sodium channel,<sup>3,4</sup> all other mutations produce a gain of function.<sup>1</sup> For proper physiologic function, sodium channels transit through closed, open, fast-inactivated, and slow-inactivated states.<sup>5</sup> All mutations producing a gain of function impair fast inactivation in a manner such that pathologic sodium current ( $I_{Na}$ ) decays more slowly or not completely, recovers faster from fast inactivation, or shows a positive shift in steady-state fast inactivation voltage-dependence.<sup>1</sup> Such gating defects determine myotonia by increasing sarcolemma excitability. Other defects may play a role in the phenotypic determination. For instance, defective

slow inactivation could contribute to the occurrence of episodic weakness.<sup>6</sup>

Mexiletine is a sodium channel blocker related to local anesthetic (LA) drugs that is usually effective in controlling myotonia in PMC and PAM but does not prevent the attacks of weakness in hyperPP.<sup>7</sup> The reason for the lack of benefit in hyperPP patients remains unclear but we proposed in a previous study that the drug may be unable to block the hyperPP-characteristic persistent late inward sodium current that depolarizes the fiber and induces paralysis.<sup>8</sup> Conversely, the singular use-dependent block of  $I_{Na}$  by LA, which occurs during repetitive depolarization owing to the higher binding affinity to activated or inactivated channels, provides the basis for the selective action of these drugs on pathologic membrane characterized by excessive firing of action potentials, with consequent anticonvulsant, antiarrhythmic, and antimyotonic properties in nerve, heart, and skeletal muscle.<sup>9,10</sup> All sodium channels present in these tissues share a common molecular LA binding site that lies within the pore.<sup>11–15</sup> The differences in LA sensitivity between sodium channel subtypes have been interpreted as structural dif-

From the Unit of Pharmacology (Drs. Desaphy, De Luca, Tortorella, and Conte Camerino), Department of Pharmaco-Biology (Dr. De Vito), Faculty of Pharmacy, University of Bari, Italy; and Division of Genetic Medicine (Dr. George), Vanderbilt University, Nashville, TN.

J.F.D. received a postdoctoral fellowship from Telethon-Italy. D.C.C. was supported by Telethon-Italy grant 1208. A.L.G. was supported by the NIH grant NS32387.

Received April 16, 2001. Accepted in final form July 21, 2001.

Address correspondence and reprint requests to Dr. Diana Conte Camerino, Unità di Farmacologia, Dipartimento Farmaco-Biologico, Facoltà di Farmacia, Università di Bari, via Orabona 4–Campus, 70125 Bari, Italy; e-mail: conte@farmbiol.uniba.it

ferences in the LA receptor site<sup>16-18</sup> or as differences in channel gating that secondarily affect drug effect.<sup>19,20</sup> A few studies have shown that LA sensitivity can differ between mutant and wild-type hSkM1 channels.<sup>21-23</sup> Defining mutant-specific pharmacology may represent a great opportunity to target therapy more precisely in individual myotonic patients.<sup>24</sup>

In the current study, we tested mexiletine and a potent derivative, Me7,<sup>25</sup> on three mutant hSkM1 channels transiently expressed in tsA201 cells. The three mutations are located in molecular domains directly involved in the fast inactivation process. The PMC mutation, R1448C, is part of the voltage sensor associated with fast inactivation; the PAM mutation, G1306E, is located within the inactivation gate that occludes the pore during depolarization; the hyperPP mutation, A1156T, is close to a putative docking site for the inactivation gate in the inactivated state.

**Methods.** *Transient expression of hSkM1 and mutants.* Full-length mutant hSkM1 constructs in the mammalian expression vector pRc/CMV were constructed as previously described,<sup>26</sup> and introduced into tsA201 cells, a cell line derivative from human embryonic kidney (HEK) cells, by transient transfection using the calcium phosphate coprecipitation method.<sup>27</sup> We transfected cells only with the  $\alpha$ -subunit of sodium channels, as the auxiliary  $\beta$ 1-subunit is endogenously expressed in HEK and tsA201 cells.<sup>28,29</sup> In fact, coexpression of  $\beta$ 1-subunit with the  $\alpha$ -subunit in HEK cells does not modify substantially the gating properties of sodium channel mutants.<sup>30</sup> Cells were cotransfected with 10  $\mu$ g of plasmid DNA encoding channel and 4  $\mu$ g of plasmid DNA encoding CD8 receptors, and were replated in 35-mm culture dishes 15 hours after transfection. Before patch clamp recording (36 to 72 hours after transfection), cells were briefly incubated with Dynal microbeads coated with anti-CD8 antibody (Dynal A.S., Oslo, Norway) to identify transfected cells.

*Electrophysiologic recordings.* Sodium currents were recorded at room temperature (20 to 22 °C) using the whole-cell patch-clamp technique. The bath solution contained (in mM) 150 NaCl, 4 KCl, 2 CaCl<sub>2</sub>, 1 MgCl<sub>2</sub>, 5 HEPES, and 5 glucose, and the pH was set to 7.4 with NaOH. The pipette solution contained (in mM) 120 CsF, 10 CsCl, 10 NaCl, EGTA (ethylene glycol bis [ $\beta$ -amino ethyl ether]-N,N,N',N'-tetraacetic acid), and 5 HEPES (N-2-hydroxyethyl piperazine-N'-2-ethane-sulfonic acid), and the pH was set to 7.2 with CsOH. Pipettes with resistance ranging from 1 to 2 M $\Omega$  were made from Corning 7052 glass (Garner glass, Claremont, CA) with a vertical puller (PP-82, Narishighe, Tokyo, Japan) and heat-polished on a microforge (MF-83, Narishighe). Currents were recorded with an Axopatch 1D amplifier (Axon Instruments, Foster City, CA). Voltage clamp protocols and data acquisition were performed with pCLAMP 6.0 software (Axon Instruments) through a 12-bit A/D/D-A interface (Digidata 1200, Axon Instruments). Currents were low-pass filtered at 2 kHz (-3 dB) by the four pole Bessel filter of the amplifier and digitized at 10 to 20 kHz.

After rupturing the patch membrane, a 25-ms-long test pulse to -20 mV from a holding potential of -120 mV was applied to the cell repetitively (0.33 Hz) until stabilization of  $I_{Na}$  amplitude and kinetics was achieved (typically 5

minutes). Data were considered for analysis only from cells exhibiting peak current amplitudes of 0.6 to 6 nA and series resistance errors <5 mV. Little (<5%) or no run-down was observed within the experiments. Specific voltage protocols are described in the Results section. Using the F value ( $p < 0.05$ ) that compares the sum of squared errors of the different fitting models,  $I_{Na}$  decay of R1448C and G1306E channel mutants was best fit with a two-exponential function including a residual current ( $R$ ):

$$I(t) = P \cdot \exp(-t/\tau_{fast}) + Q \cdot \exp(-t/\tau_{slow}) + R$$

Although a single exponential function was often significantly sufficient to fit  $I_{Na}$  decay for WT and A1156T, we used the same equation as for R1448C and G1306E to allow direct comparison. Steady-state availability was fit with the Boltzmann equation:

$$I/I_{max} = \{1 + \exp[(V - V_h)/k]\}^{-1}$$

where  $V_h$  is the half-maximum inactivation potential and  $k$  is the slope factor. Data are shown as fitted parameter  $\pm$  SE of the fit or mean  $\pm$  SEM, and  $n$  represents the number of the cells examined. Statistical difference between the means was evaluated using unpaired Student's  $t$ -test, with  $p < 0.05$  considered as significant. The R(-)-enantiomers of mexiletine and Me7 ( $\alpha$ -[(2-methylphenoxy)methyl]-benzenemethanamine) were synthesized in our laboratories as previously described.<sup>25,31</sup> The drugs were dissolved in a bath solution and applied at final concentration near the patched cell through a plastic capillary. Tonic block was measured 3 minutes after drug application using a stimulation frequency of 0.33 Hz, while use-dependent block was measured using a frequency stimulation of 10 Hz. A maximum of two drug concentrations was tested in individual cells, and data from a minimum of 3 cells were averaged at each concentration to construct concentration-response curves. The experimental points were first fit with the Hill binding function:

$$I_{drug}/I_{control} = 1/[1 + ([drug]/IC_{50})^h]$$

where  $IC_{50}$  is the half-maximum inhibitory concentration and  $h$  is the logistic slope factor. The number of data in the fit was considered sufficient when  $0.75 < h < 1.25$ , otherwise other data were collected. Finally, the curves were fit with a first-order equation ( $h$  fixed to unity) to calculate the  $IC_{50}$  values reported in the text.

**Results.** *Different effects of mutations on hSkM1 inactivation kinetics and steady-state voltage dependence.* Wild-type hSkM1 channels and the three mutants, A1156T, G1306E, and R1448C, were transiently expressed in tsA201 cells and the resulting  $I_{Na}$  were recorded with patch clamp technique in the whole-cell mode. Compared to the WT  $I_{Na}$ , the PMC R1448C mutant  $I_{Na}$  and the PAM G1306E mutant  $I_{Na}$  decayed more slowly, while the hyperPP A1156T mutant  $I_{Na}$  exhibited a persistent late component (figure 1A). Decay of  $I_{Na}$  at -20 mV was fit with a two-exponential function (see figure 1B). The slow exponential component ( $\tau_{slow}$ ) represented less than 1% of the total decay for WT and A1156T  $I_{Na}$ . For A1156T, only the fast exponential time constant ( $\tau_{fast}$ ) was slightly but significantly longer than that of WT. For R1448C and

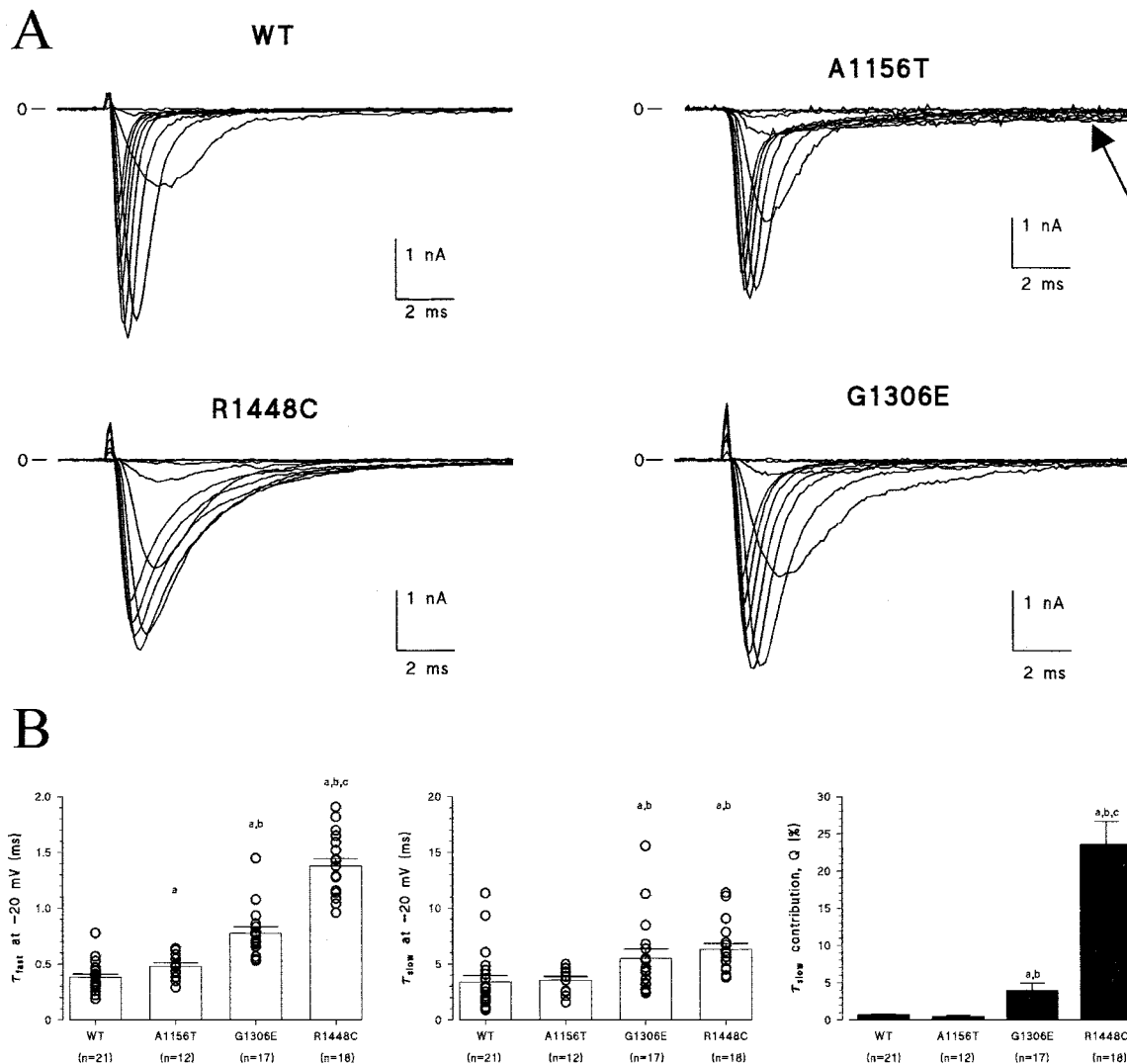


**Figure 1.** Effect of mutations on *hSkM1* channel kinetics transiently expressed in *tsA201* cells. (A) Sodium currents were recorded in the whole-cell configuration of patch-clamp technique 36 to 72 hours after transfection. Cell membrane potential was held to  $-120$  mV and 50-ms-long depolarizing pulses were applied every 3 seconds to potentials ranging from  $-80$  to  $+10$  mV. (B) Decay of sodium currents at  $-20$  mV was fit with a two-exponential function calculating two time constants, the fast exponential time constant ( $\tau_{fast}$ ) and slow exponential component ( $\tau_{slow}$ ). The bars represent the mean  $\pm$  SEM of individual  $\tau_{fast}$  and  $\tau_{slow}$  values (open circles) calculated in *n* cells, as well as the mean  $\pm$  SEM of *Q* values (the contribution of  $\tau_{slow}$  to total decay) calculated in the same cells. Unpaired Student's *t*-test between means of data revealed at least  $p < 0.05$  vs wild-type (WT) (a), A1156T (b), and G1306E (c).

G1306E, both  $\tau_{fast}$  and  $\tau_{slow}$  were dramatically prolonged and the contribution of  $\tau_{slow}$  to the decay was significantly increased, with these effects being more pronounced for R1448C.

Voltage-dependence of steady-state inactivation was measured in all the patches using a conventional double-pulse voltage protocol (figure 2A). Because of the spontaneous shift of voltage dependence classically encountered in whole cell recordings,<sup>32</sup> we took care to measure this parameter at the same time,  $\sim 10$  minutes after whole-cell configuration was achieved. WT and A1156T  $I_{Na}$  steady-state inactivation strictly presented the same voltage dependence, as shown by the superposition of Boltzmann distributions (see figure 2A). Steady-state inactivation of G1306E  $I_{Na}$  was shifted toward less negative potentials by 13 mV. In contrast, steady-state inactivation of R1448C  $I_{Na}$

was shifted in the opposite direction by 11 mV and the slope factor was increased to 14 mV from the value of about 8 mV found for WT, A1156T, and G1306E (see figure 2A).

Different sensitivity of WT and mutant sodium channels to mexiletine and its derivative Me7 at the holding potential of  $-120$  mV. Tonic block of sodium channels by the drugs was assayed 3 minutes after drug application by measuring the reduction of  $I_{Na}$  elicited from  $-120$  to  $-20$  mV at a stimulation frequency of 0.33 Hz. Figure 3A presents illustrated examples of current traces recorded before (control) and after application of mexiletine. For both WT and A1156T channels, 100  $\mu$ M mexiletine reduced peak  $I_{Na}$  by about 25% and 300  $\mu$ M mexiletine blocked 50% of the channels. The same drug concentrations had typically a twofold lower effect on peak  $I_{Na}$  of G1306E mutant. In contrast, 10-fold lower concentrations of mexil-

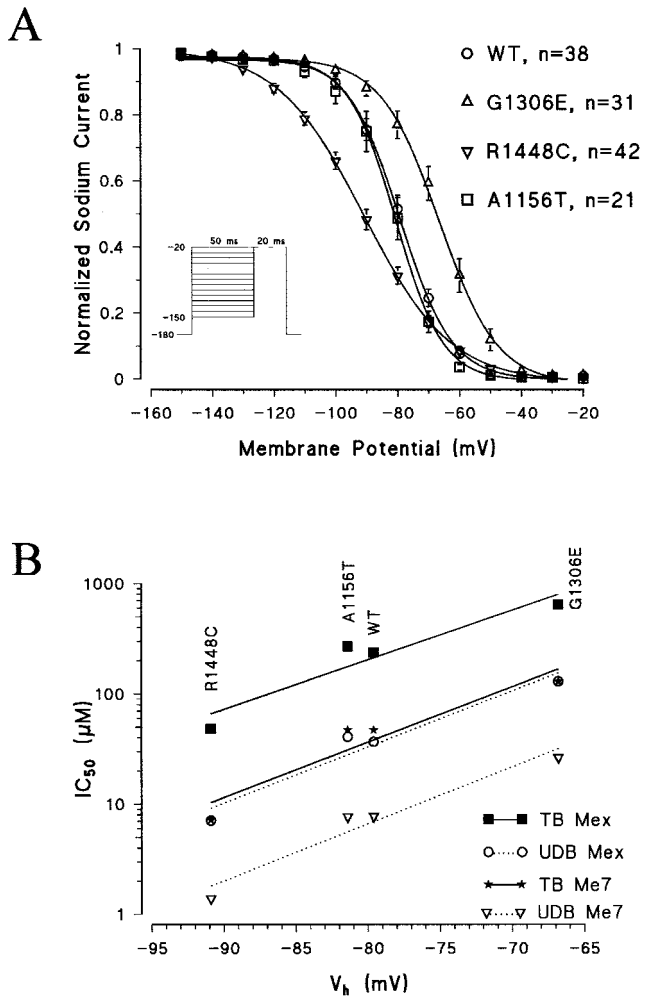


**Figure 2.** Relationships between mexiletine and Me7 half-maximum inhibitory values ( $IC_{50}$ ) determined at the holding potential of  $-120$  mV and the half-maximum inactivation potentials of sodium channel mutants. (A) Voltage dependence of steady-state fast inactivation of wild-type (WT) and mutant hSkM1 channels. Sodium currents were evoked by a 20-ms-long test pulse to  $-20$  mV after 50-ms-long conditioning pulses between  $-150$  and  $-20$  mV in 10-mV increments. Pulses were delivered at 10-ms intervals and holding potential was  $-180$  mV. The currents were normalized with respect to the maximal current and means  $\pm$  SEM were calculated from  $n$  cells to be plotted against the conditioning potential and fit with the Boltzmann equation described in Material and Methods. The calculated half-maximum inactivation potentials,  $V_{h/2}$ , along with the SE of the fit were  $-79.3 \pm 0.2$  mV for WT ( $n = 38$ ),  $-80.6 \pm 0.5$  mV for A1156T ( $n = 21$ ),  $-66.5 \pm 0.5$  mV for G1306E ( $n = 31$ ), and  $-90.9 \pm 0.3$  mV for R1448C ( $n = 44$ ). The slope factors were  $8.4 \pm 0.2$  mV for WT,  $7.6 \pm 0.4$  mV for A1156T,  $9.4 \pm 0.4$  mV for G1306E, and  $14.0 \pm 0.3$  mV for R1448C. (B) The  $IC_{50}$  for tonic block (TB) and use-dependent block (UDB) by mexiletine (Mex) and Me7 of WT and mutant channels were obtained from curve fitting of the concentration-response relationships shown in figures 3 and 4, and were reported as a function of the half-maximum inactivation potentials  $V_{h/2}$  determined from the Boltzmann fits shown in panel A. Lines show linear regression of experimental data points ( $p < 0.05$ ).

etine produced a similar block of R1448C peak  $I_{Na}$  as compared to WT. The fit of concentration-response curves with a first-order binding function indicated half-maximum concentrations ( $IC_{50}$ ) of  $236 \mu\text{M}$  for WT channels,  $269 \mu\text{M}$  for A1156T mutants,  $642 \mu\text{M}$  for G1306E mutants, and  $48 \mu\text{M}$  for R1448C mutants (see figure 3B).

Due to high binding affinities of local anesthetic-like drugs to activated or inactivated sodium channels, the block of peak  $I_{Na}$  presents use-dependent properties, such as the higher the frequency of membrane depolarization, the greater is the block. In the absence of drug, depolarizing the cell membrane from  $-120$  to  $-20$  mV at a frequency of 10 Hz produced little or no reduction of WT and mutant peak  $I_{Na}$ , indicating that such a frequency allowed a complete recovery from inactivation between depolarizing pulses. In the presence of mexiletine, use-dependent block developed rapidly toward a steady-state level as stimulation frequency was increased. At  $100 \mu\text{M}$ , mexiletine reduced WT peak  $I_{Na}$  by 80% at 0.33 Hz (tonic block), 50% at 1 Hz, 70% at 2 Hz, and 90% at 10 Hz. Concentration-response curves for use-dependent block of peak  $I_{Na}$  by mexiletine were constructed for all channels at 10 Hz (see figure 3C). The use-dependent sensitivities to mexiletine were similar for WT channels ( $IC_{50} \sim 37 \mu\text{M}$ ) and A1156T mutants ( $IC_{50} \sim 41 \mu\text{M}$ ). In contrast, the curves were shifted in opposite directions for G1306E ( $IC_{50} \sim 130 \mu\text{M}$ ) and R1448C ( $IC_{50} \sim 7 \mu\text{M}$ ) mutants.

Tonic and use-dependent block of peak current were measured in the presence of a potent derivative of mexiletine (Me7) with a phenyl group in lieu of the methyl group on the chiral carbon atom and a methyl group lacking on the aromatic moiety of the drug (figure 4A). As for mexiletine, WT and A1156T channels undergo very similar tonic ( $IC_{50} \sim 47 \mu\text{M}$ ) and use-dependent ( $IC_{50} \sim 8 \mu\text{M}$ ) block in presence of Me7 (see figure 4, B and C). Compared to WT, R1448C channels were more sensitive to Me7, with  $IC_{50}$  values of  $7 \mu\text{M}$  for tonic block and  $1.4 \mu\text{M}$  for use-dependent block. In contrast, G1306E mutants were less sensitive to Me7 than WT channels, with  $IC_{50}$  values of  $130 \mu\text{M}$  for tonic block and  $27 \mu\text{M}$  for use-dependent block.

In summary, from the holding potential of  $-120$  mV, tonic and use-dependent block of WT and mutant sodium channels by both mexiletine and Me7 followed the potency order rank R1448C > WT  $\approx$  A1156T > G1306E. Moreover, Me7 was about fivefold more potent than mexiletine in blocking all channels.

**State-dependent affinities of WT and mutant sodium channels for mexiletine and its derivative Me7.** The tonic block of  $I_{Na}$  at the holding potential (hp) of  $-120$  mV probably reflects the combination of binding to resting (closed) and inactivated sodium channels.<sup>19,25</sup> Thus we hypothesized that differences in drug affinities of sodium channel mutants observed at  $-120$  mV may result from the mutant-specific differences in the proportion of closed and inactivated channels, such differences being evidenced on voltage-dependent steady-state inactivation curves (see figure 2A).

To evaluate drug-binding affinity to closed sodium channels, we constructed concentration-response curves for tonic block from an hp of  $-180$  mV (figure 5). At this potential, the entire population of WT and mutant channels should be in the closed state, ready to open in response to depolarization. In this condition, the four

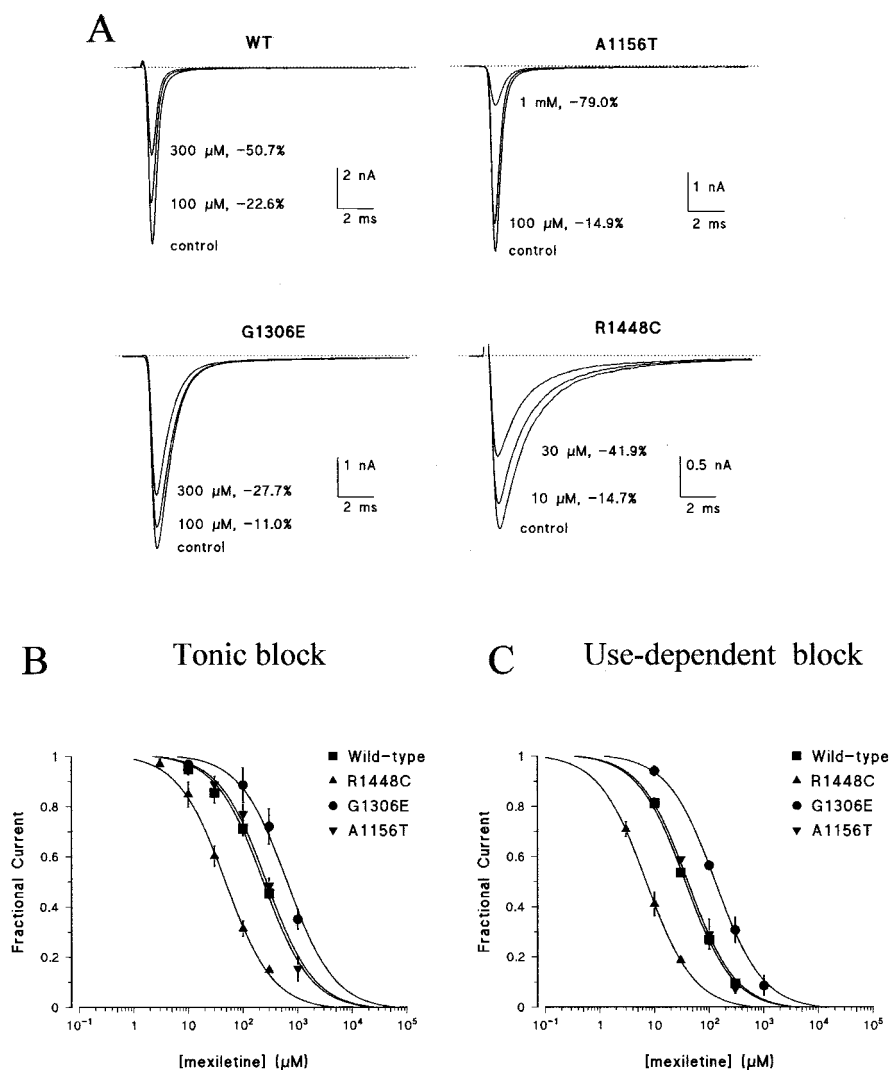


**Figure 3.** Mexiletine-induced tonic and use-dependent block of wild-type (WT) and mutant hSkM1 channels. (A) Tonic block of sodium currents ( $I_{Na}$ ) by mexiletine was assayed 3 minutes after drug application by measuring the reduction of  $I_{Na}$  elicited from  $-120$  to  $-20$  mV at a stimulation frequency of 0.33 Hz. (B) Concentration-response curves for tonic block were constructed using the protocol described in panel A and fit with the first-order binding function described in Material and Methods. The calculated half-maximum inhibitory values ( $IC_{50}$ )  $\pm$  SE of the fit were  $236 \pm 14.8$   $\mu\text{M}$  for WT,  $269 \pm 21.7$   $\mu\text{M}$  for A1156T,  $48 \pm 1.9$   $\mu\text{M}$  for R1448C, and  $642 \pm 49.4$   $\mu\text{M}$  for G1306E. (C) Concentration-response curves for use-dependent block were constructed from current amplitudes measured at the end of a 10-Hz train of test pulses ( $-120$  to  $-20$  mV) and fit with the first-order binding function described in Material and Methods. The calculated  $IC_{50}$  values  $\pm$  SE of the fit were  $37 \pm 1.3$   $\mu\text{M}$  for WT,  $41 \pm 2.5$   $\mu\text{M}$  for A1156T,  $7.1 \pm 0.1$   $\mu\text{M}$  for R1448C, and  $130 \pm 4.5$   $\mu\text{M}$  for G1306E.

channels had similar sensitivities to mexiletine ( $IC_{50} \sim 800$   $\mu\text{M}$ ) and to Me7 ( $IC_{50} \sim 130$   $\mu\text{M}$ ).

Also the use-dependent block measured from an hp of  $-180$  mV was quite similar for all channel types for mexiletine ( $IC_{50} \sim 250$   $\mu\text{M}$ ) and Me7 ( $IC_{50} \sim 45$   $\mu\text{M}$ ) (see figure 5). Because mexiletine is a very poor open-channel blocker, use-dependent block results mostly from drug binding to inactivated channels.<sup>33,34</sup> Therefore, the current data strongly suggest that the binding affinities for inactivated channels are the same for WT and mutant channels. Although it is difficult to calculate exact values, use-dependent block of R1448C mutants from the hp of  $-120$  mV further suggests that binding affinity to inactivated hSkM1 channels is lower than  $7$   $\mu\text{M}$  for mexiletine and  $1$   $\mu\text{M}$  for Me7 (see figures 3 and 4).

A new mechanism of sodium channel block by the antiarrhythmic drug lidocaine was described for the cardiac R1623Q mutant that is responsible for the long-QT syndrome.<sup>35</sup> These authors proposed that the mutation favors closed-state inactivation, that is the mutant channels have a propensity to inactivate without ever opening, and that lidocaine further increases this behavior, which results in a speed of current decay rate. Because the arginine in position 1623 of the cardiac sodium channel corresponds to the arginine in position 1448 of the hSkM1 channel, we

looked at the effects of mexiletine and Me7 on  $I_{Na}$  kinetics. Control  $I_{Na}$ , drug-modified  $I_{Na}$ , and drug-modified  $I_{Na}$  normalized with respect to peak control  $I_{Na}$  (dashed lines) are presented in figure 6. This analysis was performed for  $I_{Na}$  elicited from either  $-120$  or  $-180$  mV and for drug concentrations close to the  $IC_{50}$  value respective to each channel type. Drugs produced no kinetic change for WT and A1156T  $I_{Na}$  from either hp (data not shown). No effect was observed also for R1448C and G1306E mutant  $I_{Na}$  elicited from  $-120$  mV (data not shown). In contrast, higher concentrations of mexiletine and Me7 accelerated the decay rate of R1448C and G1306E mutant  $I_{Na}$  elicited from  $-180$  mV (see figure 6A). Using the fitting routine described above (see figure 1), we found that the drugs did not modify  $\tau_{fast}$  and  $\tau_{slow}$  values, but dramatically reduced the contribution of  $\tau_{slow}$  to  $I_{Na}$  decay (see figure 6B). Such effect tended to occur at the hp of  $-120$  mV but no statistical difference was reached, which may explain the difficulty to note it by simply superposing control  $I_{Na}$  and normalized drug-modified  $I_{Na}$ .

**Discussion.** Patients carrying sodium channel mutations generally experience a significant improvement in control of myotonia following daily

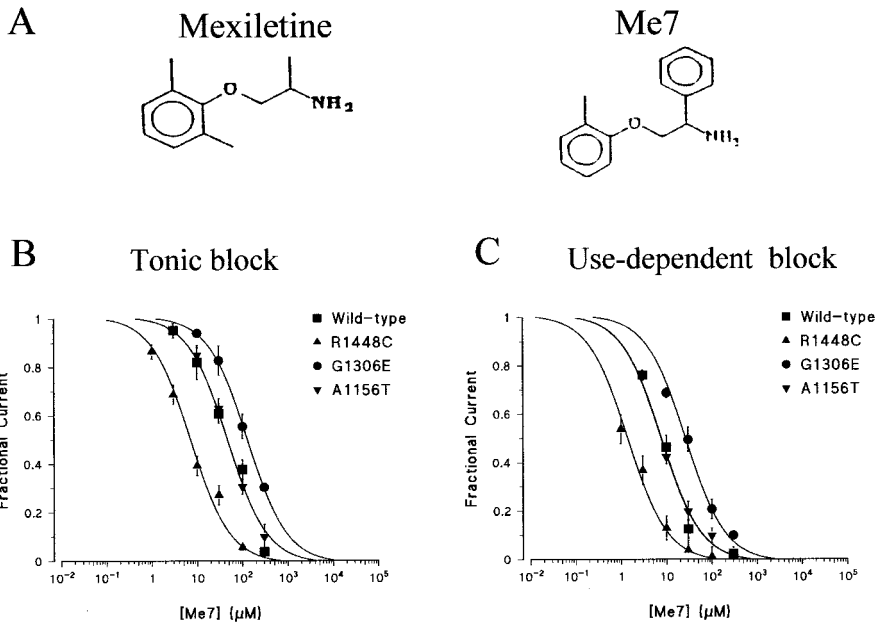


Figure 4. Me7-induced tonic and use-dependent block of wild-type (WT) and mutant hSkM1 channels. (A) Chemical structure of mexiletine and the derivative, Me7. (B) Concentration-response curves for tonic block of WT and mutant hSkM1 currents were constructed and fit as described in figure 3B. The calculated  $IC_{50}$  values  $\pm$  SE of the fit were  $47 \pm 5.5 \mu\text{M}$  for WT,  $47 \pm 3.0 \mu\text{M}$  for A1156T,  $7.2 \pm 0.7 \mu\text{M}$  for R1448C, and  $130 \pm 2.8 \mu\text{M}$  for G1306E. (C), Concentration-response curves for use-dependent block of wild-type and mutant hSkM1 currents were constructed and fit as described in figure 3C. The calculated  $IC_{50}$  values  $\pm$  SE of the fit were  $7.8 \pm 0.8 \mu\text{M}$  for WT,  $7.7 \pm 0.4 \mu\text{M}$  for A1156T,  $1.4 \pm 0.1 \mu\text{M}$  for R1448C, and  $27 \pm 1.8 \mu\text{M}$  for G1306E.

treatment with the sodium channel blocker, mexiletine.<sup>7</sup> Yet we observed that when assayed from an hp of  $-120 \text{ mV}$ , mexiletine inhibits  $I_{\text{Na}}$  flowing through WT and mutant channels with different potencies following the order rank R1448C > WT  $\approx$  A1156T > G1306E. This could be theoretically interpreted as a mutant-specific structural difference in mexiletine receptor or as a mutant-specific gating difference underlying apparent difference in mexiletine affinity. Yet our results demonstrate that mutations do not modify state-dependent affinities, indicating no alteration of the receptor site for mexiletine. Moreover, none of the amino acids known to constitute the putative molecular receptor for LA have been linked to clinical myotonia or periodic paralysis. Therefore, channel gating differences account for the different responses of myotonic mutant hSkM1 channels to mexiletine.

Accordingly to previous studies, we found that the hyperPP A1156T mutation slightly slows  $I_{\text{Na}}$  decay rate and produces a persistent late inward current.<sup>1</sup> Such a persistent anomalous sodium current may

keep the fiber depolarized, causing the muscle weakness that characterizes hyperPP.<sup>36</sup> No appreciable persistent late current is observed with the two other mutations, but both remarkably slow the decay rate of  $I_{\text{Na}}$ , a phenomenon that may be a common feature of myotonia-causing mutations.<sup>26</sup> Moreover, the voltage dependence of G1306E channel availability is shifted positively, which certainly contributes to the pathologic mechanism of myotonia by increasing sodium channel availability at a given membrane potential. In contrast, the R1448C mutation shifts fast inactivation voltage dependence toward more negative potentials, which in principle may limit the severity of the other gating defects in producing myotonia.

What is the gating mechanism that could explain the differences in channel sensitivity to mexiletine? As shown in other recent studies evaluating LA action on different sodium channel isoforms,<sup>19,20</sup> we found that the sensitivity to mexiletine tracks with the voltage dependence of channel fast inactivation (see figure 2B). Such a relationship also applies to

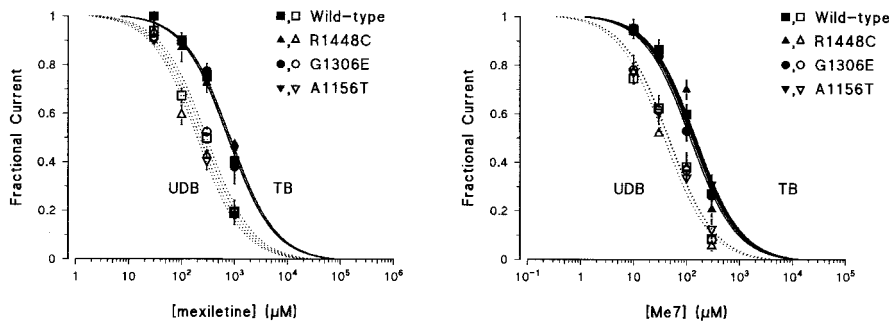
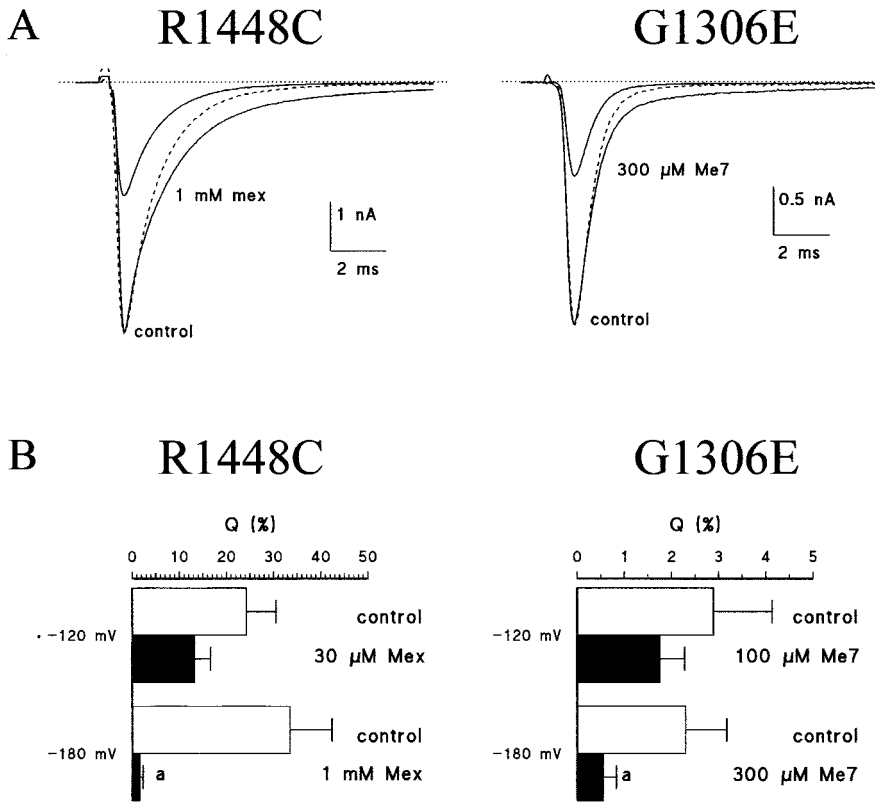


Figure 5. Tonic and use-dependent block of wild-type (WT) and mutant hSkM1 channels by mexiletine and Me7 at a holding potential of  $-180 \text{ mV}$ . Concentration-response curves were constructed as shown in figure 3, except the hp was  $-180 \text{ mV}$ . The calculated half-maximum inhibitory values ( $IC_{50}$ )  $\pm$  SE of the fit were  $767 \pm 50.5 \mu\text{M}$  (WT),  $831 \pm 35.2 \mu\text{M}$  (A1156T),  $833 \pm 51.8 \mu\text{M}$  (R1448C), and  $757 \pm 92.1 \mu\text{M}$  (G1306E) for tonic block by mexiletine;

$260 \pm 22.7 \mu\text{M}$  (WT),  $224 \pm 12.1 \mu\text{M}$  (A1156T),  $199 \pm 24.0 \mu\text{M}$  (R1448C), and  $299 \pm 20.1 \mu\text{M}$  (G1306E) for use-dependent block by mexiletine;  $139 \pm 9.9 \mu\text{M}$  (WT),  $130 \pm 9.1 \mu\text{M}$  (A1156T),  $150 \pm 29.1 \mu\text{M}$  (R1448C), and  $118 \pm 6.1 \mu\text{M}$  (G1306E) for tonic block by Me7; and  $47 \pm 6.4 \mu\text{M}$  (WT),  $46 \pm 3.3 \mu\text{M}$  (A1156T),  $39 \pm 5.8 \mu\text{M}$  (R1448C), and  $47 \pm 4.8 \mu\text{M}$  (G1306E) for use-dependent block by Me7.



**Figure 6.** Effects of mexiletine (Mex) and Me7 on current decay rate of R1448C and G1306E mutant hSkM1 channels. (A) Sodium currents ( $I_{Na}$ ) were evoked by 25-ms-long test pulses to  $-20$  mV applied at 0.33 Hz from the hp of  $-180$  mV before (control) and after application of drugs at concentrations close to the relative half-maximum inhibitory values ( $IC_{50}$ ).  $I_{Na}$  measured during drug exposure was scaled with respect to peak amplitude of control  $I_{Na}$  (dashed line). (B) Fit parameters, the fast exponential time constant ( $\tau_{fast}$ ), slow exponential component ( $\tau_{slow}$ ), and  $Q$  were calculated as described in figure 1. Each bar represents the mean  $\pm$  SEM of results obtained in at least four cells. Statistical analysis was performed using paired Student's  $t$ -test. \*Indicates  $p < 0.05$  vs control.

the other mutations studied so far, which are the hyperPP M1360V and the PMC R1448H, F1473S, and T1313M.<sup>21-23</sup> Accordingly to the modulated receptor hypothesis,<sup>9,10</sup> this phenomenon could be attributed to the high binding affinity of the drug to fast inactivated channels. Yet, by virtue of the coupling of fast inactivation with activation and slow inactivation,<sup>37-39</sup> this model was recently challenged and it is now proposed that alteration of activation or slow inactivation may secondarily affect the fast inactivation process of the channel.<sup>20,40</sup> Our results allow to exclude the involvement of slow inactivation in the pharmacologic differences between myotonic channels, as this property does not differ between wild-type channels and the three mutants studied here.<sup>6</sup> Yet, we can not discriminate between channel activation and fast inactivation responsibility in mutant-specific response to mexiletine.

Voltage dependence of channel availability may be considered as a general index of mutant channel responsiveness to drug therapy. Accordingly, patients carrying the R1448C mutation respond very well to mexiletine therapy,<sup>23</sup> probably owing to the preferential block of mutants as compared to WT channels. Patients carrying the G1306E mutation endure severe myotonia and need constant medication.<sup>41</sup> Our study suggests that the beneficial effect of mexiletine in these patients is attributable mainly to the block of WT channels. We anticipate that this mechanism applies to all mutations producing a rightward shift of the availability curve and that patients may benefit from a drug having a more specific action on the mutant channel.

A great improvement of antimyotonic therapy could be in finding drugs able to correct specifically the biophysical defect responsible for myotonia. Interestingly, we observed that a high concentration of mexiletine is able to accelerate  $I_{Na}$  decay rate of myotonic mutants toward that of WT channels. Such an effect is generally explained by open-channel block mechanism, i.e., the binding of the drug to open channels forces the channel to close prematurely. However, it is unlikely to be the case for mexiletine because this drug is not able to reduce mean open times of slowly-inactivating skeletal muscle sodium channels.<sup>33</sup> Moreover, the fact that  $\tau_{fast}$  and  $\tau_{slow}$  values remain unaltered in the presence of mexiletine argues against a potential open-channel block mechanism by these drugs. Using computer simulation, a similar effect of the related drug lidocaine on  $I_{Na}$  decay of the cardiac channel R1623Q mutant has been interpreted as the enhancement of channel inactivation from closed states by the drug.<sup>35</sup> Yet our analysis indicates that the effect of mexiletine on  $I_{Na}$  decay rate is attributable to the dramatic reduction of the contribution of  $\tau_{slow}$  to total decay. The two time constants,  $\tau_{fast}$  and  $\tau_{slow}$ , needed to describe the decay of myotonic mutant  $I_{Na}$  are the macroscopic manifestation of channels gating in a fast mode, named M1, and a slowly inactivating mode, named M2.<sup>42</sup> The M2 gating mode is largely repressed in native tissues and physiologic conditions, whereas it can be exacerbated in some situations such as in case of myotonic mutations. Thus only a high concentration of mexiletine appears to stabilize myotonic mutant channels in the M1 gating mode, which may

represent a specific therapeutic approach toward sodium channel myotonias.

According to the effects of Me7 and closely related mexiletine derivatives on native sodium channels in frog and rat muscle fibers, Me7 is more potent than the parent mexiletine in blocking human sodium channels heterologously expressed in a mammalian cell line.<sup>25,33</sup> Such improvement probably results from the increased hindrance on the chiral carbon atom of the drug due to the presence of the phenyl group, and the lesser stringency on the aromatic moiety of the molecule due to the absence of one methyl group. In addition, Me7 inhibits channels in the M2 gating mode at lower concentration than mexiletine. Thus, Me7 appears to be a good candidate to improve the antimyotonic therapy in sodium channelopathies, especially in case of patient resistance to mexiletine therapy.

## References

1. Cannon SC. Voltage-gated ion channelopathies of the nervous system. *Clin Neurosci Res* 2001;57:772–779.
2. Bulman DE, Scoggan KA, van Oene MD, et al. A novel sodium channel mutation in a family with hypokalemic periodic paralysis. *Neurology* 1999;53:1932–1936.
3. Struyk AF, Scoggan KA, Bulman DE, Cannon SC. The human skeletal muscle Na channel mutation R669H associated with hypokalemic periodic paralysis enhances slow inactivation. *J Neurosci* 2000;20:8610–8617.
4. Jurkat-Rott K, Mitrovic N, Hang C, et al. Voltage-sensor sodium channel mutations cause hypokalemic periodic paralysis type 2 by enhanced inactivation and reduced current. *Proc Natl Acad Sci USA* 2000;97:9549–9554.
5. Marban E, Yamagishi T, Tomaselli GF. Structure and function of voltage-gated sodium channels. *J Physiol* 1998;508:647–657.
6. Hayward LJ, Sandoval GM, Cannon SC. Defective slow inactivation of sodium channels contributes to familial periodic paralysis. *Neurology* 1999;52:1447–1453.
7. Moxley RT. Channelopathies. *Curr Treatment Opt Neurol* 2000;2:31–47.
8. Desaphy J-F, Conte Camerino D, Tortorella V, De Luca A. Effect of mexiletine on sea anemone toxin-induced noninactivating sodium channels of rat skeletal muscle, a model of sodium channel myotonia. *Neuromuscul Disord* 1999;9:182–189.
9. Hille B. Local anesthetics: hydrophilic and hydrophobic pathways for the drug-receptor reaction. *J Gen Physiol* 1977;69:497–515.
10. Hondeghem LM, Katzung BG. Time- and voltage-dependent interactions of the antiarrhythmic drugs with cardiac sodium channels. *Biochim Biophys Acta* 1977;472:373–398.
11. Ragsdale DS, McPhee JC, Scheuer T, Catterall WA. Molecular determinants of state-dependent block of Na<sup>+</sup> channels by local anesthetics. *Science* 1994;265:1724–1728.
12. Sunami A, Dudley SC, Fozzard HA. Sodium channel selectivity filter regulates antiarrhythmic drug binding. *Proc Natl Acad Sci USA* 1997;94:14126–14131.
13. Nau C, Wang S-Y, Strichartz GR, Wang GK. Point mutations at N434 in D1-S6 of  $\mu$ 1 Na<sup>+</sup> channels modulate binding affinity and stereoselectivity of local anesthetic enantiomers. *Mol Pharmacol* 1999;56:404–413.
14. Wang S-Y, Nau C, Wang GK. Residues in Na<sup>+</sup> channel D3-S6 segment modulate both batrachotoxin and local anesthetic affinities. *Biophys J* 2000;79:1379–1387.
15. Yarov-Yarovoy V, Brown J, Sharp EM, Clare JJ, Scheuer T, Catterall WA. Molecular determinants of voltage-dependent gating and binding of pore-blocking drugs in transmembrane segment IIIS6 of the Na<sup>+</sup> channel  $\alpha$ -subunit. *J Biol Chem* 2001;276:20–27.
16. Nuss HB, Tomaselli GF, Marban E. Cardiac sodium channels (hH1) are intrinsically more sensitive to tonic block by lidocaine than are skeletal muscle ( $\mu$ 1) channels. *J Gen Physiol* 1995;106:1193–1210.
17. Wang DW, Nie L, George AL, Bennett PB. Distinct local anesthetic affinities in Na<sup>+</sup> channel subtypes. *Biophys J* 1996;70:1700–1708.
18. Weiser T, Qu Y, Catterall WA, Scheuer T. Differential interaction of *R*-mexiletine with the local anesthetic receptor site on brain and heart sodium channel  $\alpha$ -subunits. *Mol Pharmacol* 1999;56:1238–1244.
19. Wright SN, Wang S-Y, Kallen RG, Wang GK. Differences in steady-state inactivation between Na channel isoforms affect local anesthetic binding affinity. *Biophys J* 1997;73:779–788.
20. Nuss HB, Kambouris NG, Marban E, Tomaselli GF, Balsler JR. Isoform-specific lidocaine block of sodium channels explained by differences in gating. *Biophys J* 2000;78:200–210.
21. Fan Z, George AL Jr, Kyle JW, Makielski JC. Two human paramyotonia congenita mutations have opposite effects on lidocaine block of Na<sup>+</sup> channels expressed in a mammalian cell line. *J Physiol* 1996;496:275–286.
22. Fleischhauer R, Mitrovic N, Deymeer F, Lehmann-Horn F, Lerche H. Effect of temperature and mexiletine on the F1473S Na<sup>+</sup> channel mutation causing paramyotonia congenita. *Pflügers Arch* 1998;436:757–765.
23. Weckbecker K, Wurz A, Mohammadi B, et al. Different effects of mexiletine on two mutant sodium channels causing paramyotonia congenita and hyperkalemic periodic paralysis. *Neuromuscul Disord* 2000;10:31–39.
24. Griggs RC, Ptáček LJ. Mutations of sodium channels in periodic paralysis. Can they explain the disease and predict treatment? *Neurology* 1999;52:1309–1310.
25. De Luca A, Natuzzi F, Desaphy J-F, et al. Molecular determinants of mexiletine structure for potent and use-dependent block of skeletal muscle sodium channels. *Mol Pharmacol* 2000;57:268–277.
26. Yang N, Ji S, Zhou M, et al. Sodium channel mutations in paramyotonia congenita exhibit similar biophysical phenotypes in vitro. *Proc Natl Acad Sci USA* 1994;91:12785–12789.
27. Cannon SC, Strittmatter SM. Functional expression of sodium channel mutations identified in families with periodic paralysis. *Neuron* 1993;10:317–326.
28. Moran O, Nizzari M, Conti F. Endogenous expression of the  $\beta$ 1A sodium channel subunit in HEK-293 cells. *FEBS Lett* 2000;473:132–134.
29. Malhotra JD, Chen C, Rivolta I, et al. Characterization of sodium channel  $\alpha$ - and  $\beta$ -subunits in rat and mouse cardiac myocytes. *Circulation* 2001;103:1303–1310.
30. Hayward LJ, Brown RH Jr, Cannon SC. Inactivation defects caused by myotonia-associated mutations in the sodium channel III-IV linker. *J Gen Physiol* 1996;107:559–576.
31. Franchini C, Celluci C, Corbo F, et al. Stereospecific synthesis and absolute configuration of mexiletine. *Chirality* 1994;6:590–595.
32. Wang DW, George AL Jr, Bennett PB. Comparison of heterologously expressed human cardiac and skeletal muscle Na<sup>+</sup> channels. *Biophys J* 1996;70:238–245.
33. Desaphy J-F, Conte Camerino D, Franchini C, Lentini G, Tortorella V, De Luca A. Increased hindrance on the chiral carbon atom of mexiletine enhances the block of rat skeletal muscle Na<sup>+</sup> channels in a model of myotonia induced by ATX. *Br J Pharmacol* 1999;128:1165–1174.
34. Sunami A, Fan Z, Sawanobori T, Hiraoka M. Use-dependent block of Na<sup>+</sup> currents by mexiletine at the single channel level in guinea pig ventricular myocytes. *Br J Pharmacol* 1991;110:183–192.
35. Kambouris NG, Nuss HB, Johns DC, Marban E, Tomaselli GF, Balsler JR. A revised view of cardiac sodium channel “blockade” in the long-QT syndrome. *J Clin Invest* 2000;105:1133–1140.
36. Cannon SC, Brown RH Jr, Corey DP. Theoretical reconstruction of myotonia and paralysis caused by incomplete inactivation of sodium channels. *Biophys J* 1993;65:270–288.
37. Kuo CC, Bean BP. Na<sup>+</sup> channels must deactivate to recover from inactivation. *Neuron* 1994;12:819–829.

38. Featherstone DE, Richmond JE, Ruben PC. Interaction between fast and slow inactivation in Skm1 sodium channels. *Biophys J* 1996;71:3098–3109.
39. Nuss HB, Balsler JR, Orias DW, Lawrence JH, Tomaselli GF, Marban E. Coupling between fast and slow inactivation revealed by analysis of a point mutation (F1304Q) in  $\mu$ 1 rat skeletal muscle sodium channels. *J Physiol* 1996;494:411–429.
40. Vedantham V, Cannon SC. The position of the fast-inactivation gate during lidocaine block of voltage-gated Na<sup>+</sup> channels. *J Gen Physiol* 1999;113:7–16.
41. Mitrovic N, George AL Jr, Lerche H, Wagner S, Fahlke C, Lehmann-Horn F. Different effects on gating of three myotonia-causing mutations in the inactivation gate of the human muscle sodium channel. *J Physiol* 1995;487:107–114.
42. Zhou JY, Potts JF, Trimmer JS, Agnew WS, Sigworth FJ. Multiple gating modes and the effect of modulating factors on the  $\mu$ 1 sodium channel. *Neuron* 1991;7:775–785.

---

# Effect of neurophilin ligands on motor units in mice with SOD1 ALS mutations

J.M. Shefner, MD, PhD; R.H. Brown, Jr., MD, DPhil; D. Cole, MD; P. Chaturvedi, MD; D. Schoenfeld, PhD; K. Pastuszak, BS; R. Matthews, BS; M. Upton-Rice, BS; and M.E. Cudkowicz, MD

---

**Article abstract**—*Background:* Mice with transgenes that express mutations in the gene for cytosolic copper/zinc superoxide dismutase (SOD1) develop motor neuron degeneration resembling human ALS. Neurophilin ligands are small molecules that promote neurite outgrowth. *Objective:* To test the hypothesis that treatment with two neurophilin ligands increases survival in these ALS mice by slowing the loss of motor neurons and increasing the sizes of motor units. *Methods:* Transgenic mice hemizygous for the G93A mutation were untreated or treated from 30 days of age with one of two doses of two neurophilin ligands (V-13,670; V-10,367, Vertex Pharmaceuticals, Boston, MA). Onset of behavioral abnormalities and survival were recorded. Motor unit number estimation (MUNE) was performed every 21 days starting at age 60 days. *Results:* In control animals, disease onset occurred at 77.0 days of age and death occurred at 137 days of age. Neither neurophilin ligand affected the disease course. In control animals, MUNE declined with time beginning before behavioral abnormalities were noted, and motor unit size increased concomitantly. There was no effect of drug on motor unit loss as assessed by MUNE; however, motor unit size increased more rapidly and to a greater degree in animals treated with V-13,670. *Conclusion:* As in human ALS, the transgenic ALS mice show physiologic changes in the motor unit prior to the development of clinical signs: MUNE declines as motor unit size increases. Although neither neurophilin ligand significantly affected survival, one produced an increase in motor unit size. The fact that survival was not altered by the increase in motor unit size may reflect the rapid disease course in this animal model.

NEUROLOGY 2001;57:1857–1861

---

Neurophilin ligands are small-molecule compounds that promote neurite outgrowth in vitro and improve outcomes in vivo in animal models of traumatic nerve injury, diabetic neuropathy, toxin-induced neuropathy, spinal cord injury, and PD.<sup>1–7</sup> The term *neurophilin* refers to the target or targets mediating the effects of this class of compounds, by way of analogy to the term *immunophilin*, which encompasses the endogenous targets of various immunosuppressive drugs. The identity or identities of the endogenous neurophilins have not been described. In a rat model of diabetic neuropathy, several neurophilin ligands improved nerve function,<sup>8</sup> as gauged by increases in nerve conduction velocity in both sensory and motor axons and in the density of sensory

nerve endings in skin biopsies. This latter observation suggests that neurophilin ligands may promote sprouting in distal nerve terminals. The fact that axon sprouting and nerve conduction velocities may be enhanced by neurophilin ligands suggests that these compounds might be beneficial in disorders characterized by pathology in distal nerve terminals. One such disease is ALS, a disorder in which motor neurons degenerate. Pathologic studies suggest that one component of the degenerative process in ALS is subnormal sprouting of distal motor nerve terminals.<sup>9,10</sup>

Mutations in the gene encoding cytosolic copper/zinc superoxide dismutase (SOD1) account for 25% of familial ALS (FALS).<sup>11</sup> Like patients with FALS,

From the Department of Neurology (Dr. Shefner), Upstate Medical University, Syracuse, NY; Cecil B. Day Laboratory for Neuromuscular Research (Drs. Brown and Cudkowicz, K. Pastuszak, M. Upton-Rice, and R. Matthews) and Neurology Clinical Trial Unit (Drs. Cudkowicz and Schoenfeld), Massachusetts General Hospital, Boston; and Vertex Pharmaceuticals (Drs. Cole and Chaturvedi), Boston, MA.

Supported by a grant from Vertex Pharmaceuticals, Boston, MA.

Presented in part at the annual meeting of the American Academy of Neurology; San Diego, CA; April 30–May 4, 2000.

Received October 6, 2000. Accepted in final form July 26, 2001.

Address correspondence and reprint requests to Dr. J.M. Shefner, Department of Neurology, Upstate Medical University, 750 East Adams Street, Syracuse, NY 13210; e-mail: shefnerj@upstate.edu